Proceedings of the 29th Annual International
Conference of the IEEE EMBS
Cité Internationale, Lyon, France
August 23-26, 2007.

ThP2B5.4

Segmentation of Optic Nerve Head using Warping and RANSAC

Sun Kwon Kim, Hyoun-Joong Kong, Jong-Mo Seo, Bum Joo Cho, Ki Ho Park, Jeong Min Hwang,
Dong-Myung Kim, Hum Chung and Hee Chan Kim

Abstract— **Glaucoma is the second leading cause of blindness, and the retinal nerve fiber layer (RNFL) defect is the early sign of the glaucomatous optic nerve damage. To evaluate the RNFL, segmentation of the optic nerve head on the RNFL photograph should be the first step. This paper presents segmentation of optic nerve head using warping and random sample consensus (RANSAC). Sensitivity and positive predictability of the proposed method were 91% and 78% respectively.**

I. INTRODUCTION

G LAUCOMA is the second leading cause of blindness in the world [1]. Appropriate treatment in the early stage of the glaucoma does not only save years of vision, but also reduce cost in the social perspective [2]. Visual field examination, retinal nerve fiber layer photography (RNFLP), retinal thickness analysis and stereo disc photography are used to detect the glaucomatous change. However, all of these methods need interpretation of the glaucoma specialist, requiring highly skilled, but subjective decision. Thus reliable automated analysis should be developed for mass screening of the glaucomatous optic nerve damage [3].

Measurement of RNFL thickness is useful in detecting early glaucomatous nerve fiber layer loss [4]. RNFL defect on the RNFLP correlates with the RNFL thickness of the retina, which precedes the progression of the visual field defect [5]. To evaluate the RNFL defect on the RNFLP, the brightness of the RNFL around the optic nerve head should be analyzed, thus the optic nerve head should be segmented in the first stage of the analysis.

Many papers on optic nerve head segmentation have been proposed. One of them used a freeform SNAKE and a preprocessing method to minimize incorrect boundary detection resulted from blood vessels crossing the optic nerve head [6]. Another approach proposed a modified

active shape model for segmentation of optic nerve head in their automatic feature extraction from color fundus photographs [7]. The application of morphology in color space was also proposed [8]. However, these methods are not appropriate to the RNFLP analysis, because vessels in and around optic nerve head have adverse effects on the results of those methods.

This study proposes new method for the segmentation of optic nerve head in RNFLP. The new method is based on image warping and random sample consensus (RANSAC) technique. This method provides the novel robust approach for the segmentation by the boundary modeling of optic nerve head in one-dimension.
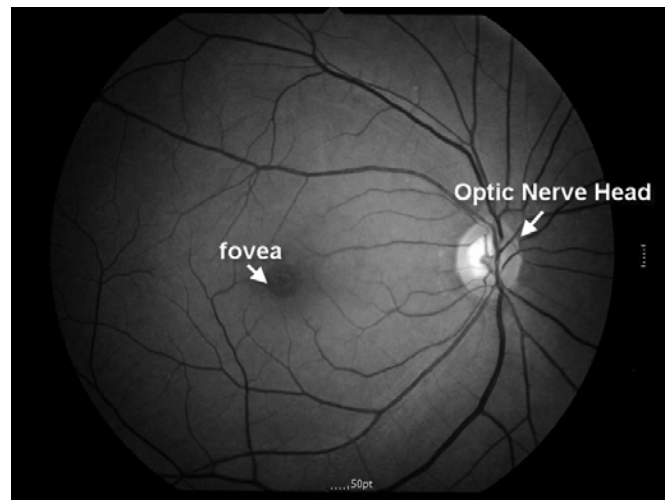

Fig. 1 Optic nerve head and fovea on the RNFL image

II. MATERIALS AND METHODS

A. Materials

RNFLPs were acquired by digital fundus camera system (CF-60UVi / D60, Cannon Inc, Tokyo, Japan) where the green filter was inserted to enhance the RNFL on the photograph in the course of the acquisition. Acquisition angle was 60° and the image was stored in 1600x1216 pixel DICOM format and transferred for further analysis. DICOM formatted images were converted to 8bit gray JPEG format images for the analysis and resized to 800 x 608 for reducing computation time.

B. Localization of optic nerve head and fovea

To localize the center of optic nerve head and that of fovea, Kong's method [9] was adopted as follows. To eliminate the speckle noises without blurring the image, median filtering was performed. And Contrast Limited

Adaptive Histogram Equalization (CLAHE) was used to enhance the image contrast locally. Sliding neighborhood operation was used to make the standard deviation image. Each pixel in the image has standard deviation value of corresponding window. After applying average filter with 180 pixel-sized windows to smooth the sharpness of the image, the brightest point is selected as the center of optic nerve head.

To find the center of the fovea, cross-correlation between median-filtered RNFLP and predefined template was calculated, and the point having maximum cross-correlation value was selected as a vicinity point of the fovea. CLAHE is performed and then the darkest point was chosen as the center of the fovea. Fig. 2 shows the results of localization of optic nerve head and fovea.

C. Warping

Imaginary circle was defined from the center of the optic nerve head, with the radius of one third of the distance between the center of optic nerve head and that of fovea. After then, the circle was warped into rectangle. Radial profiles were extracted at each 360° angles around the circle at 1° intervals from 0° through 359°. The rectangle-formed image consists of profiles of area in the circle centered at optic nerve head.

Binarization was performed by thresholding technique. Every pixel having gray-level less than the half of the total level was discarded in the image. All the pixels on each row having number of pixels less than one third width of image were removed. And only bottom pixels at each column were remained. Each step is illustrated in Fig. 3.
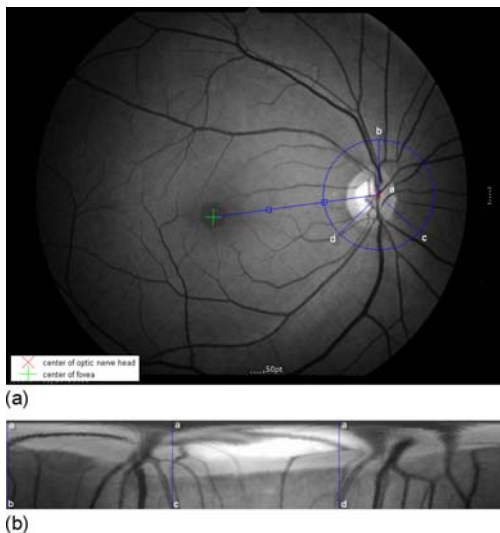
Fig. 2 (a) Localization of optic nerve head and fovea and (b) rectangle-formed image of optic nerve head
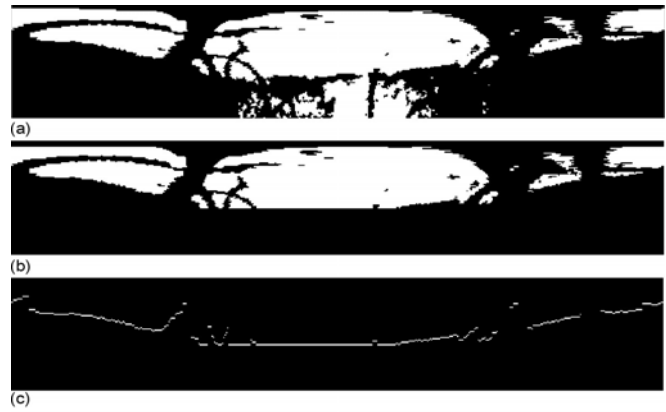
Fig. 3 (a) binarized image (b) image after discarding rows having number of pixels under one third width of image (c) image after remaining only bottom pixels at each column
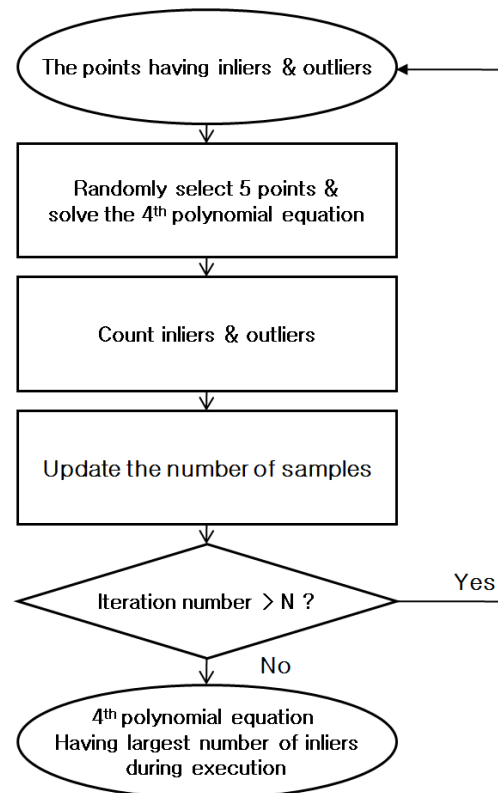
D. RANSAC

Fig. 4 Flow chart of RANSAC

RANSAC proposed by Fischler and Bolles has been generally used as an estimator in computer vision [10, 11]. RANSAC has different approach with conventional smoothing techniques. Whereas other techniques try to use as many data as possible, RANSAC initially selects only minimum data required for estimating the model. When RANSAC finds new data that are feasible for the model, those data is added to selected data. At last, all selected data are used for updating the model to minimize error between the model and selected data.

A point within threshold distance **Dth** from the model is referred to "inlier" and a point outside of that is referred to

"outlier". Equation (1) shows the function to determine whether a point is an inlier or outlier, where Y_i is a y-coordinate of the selected point and Y_i' is that of the model at the same x-coordinate with the selected point.

$$F = \begin{cases} \text{inliers}, & \text{if } \left| Y_i - Y_i' \right| < D_{th} \\ \text{outliers}, & \text{if } \left| Y_i - Y_i' \right| > D_{th} \end{cases} \tag{1}$$

In this paper, a sample for solving the model consists of five points, because the boundary of optic nerve head is assumed that it has the shape of 4th order polynomial equation as the model. And the equation is solved correctly only when there are no outliers among the points chosen. But there are inliers and outliers among the total points as shown in Fig. 3(c). To ensure the probability **p** that at least one of the random samples of five points is free from outliers, the number of samples N is chosen sufficiently high. The probability of outlier **e** is calculated by (2)

$$e = \frac{\text{number of outliers}}{\text{number of total points}} \tag{2}$$

The number of samples N is calculated by (3) and updated through the algorithm until termination. Whenever the algorithm executes N times, RANSAC process is finished.

$$N = \log(1-p)\big/\log(1-(1-e)^5) \tag{3}$$

Fig. 4 shows the overall process of RANAC and Fig. 5 illustrates the result of RANSAC. Dashed lines are boundary of area within threshold distance and a solid line between two dashed lines is the model, which represents boundary of optic nerve head.
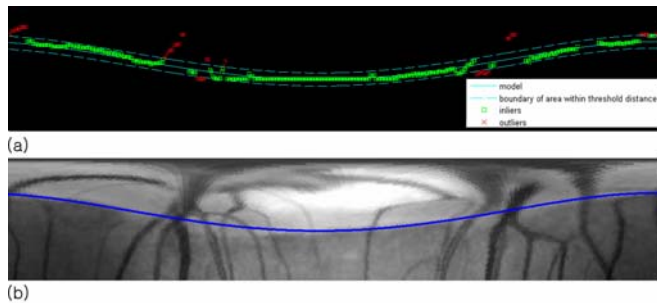

Fig. 5 (a) a result of RANSAC (b) Rectangle-formed image overlapped with the model

E. Reverse-warping

The model is warped into circle inversely. Every point of the model in the rectangle-formed image can be mapped to the original RNFLP. Fig. 6 shows the result of reverse-warping.
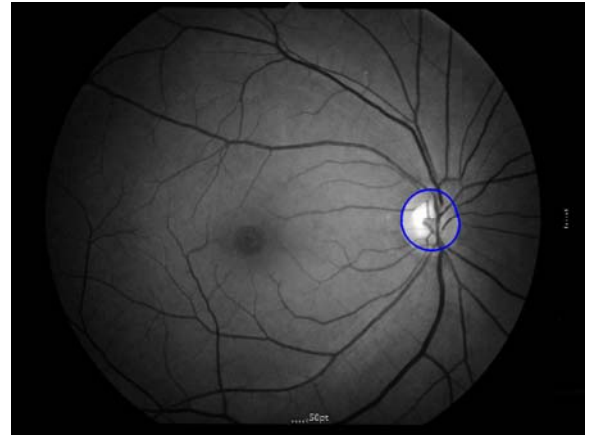

Fig. 6 Original retinal nerve fiber layer image overlapped with reverse-warped model

III. RESULT

Fifty-three normal and thirty RNFLP with glaucomatous changes were used. Fig. 7 shows the results of proposed algorithm. Segmentation of optic nerve head was performed manually by two ophthalmologists, and the mean segmented area was stored as a reference image. Performance of the algorithm was evaluated by sensitivity and positive predictability. Fig.8 shows area of true positive, true negative, false positive, and false negative. The sensitivity of the proposed method was 91±9% and positive predictability was 78±19%.
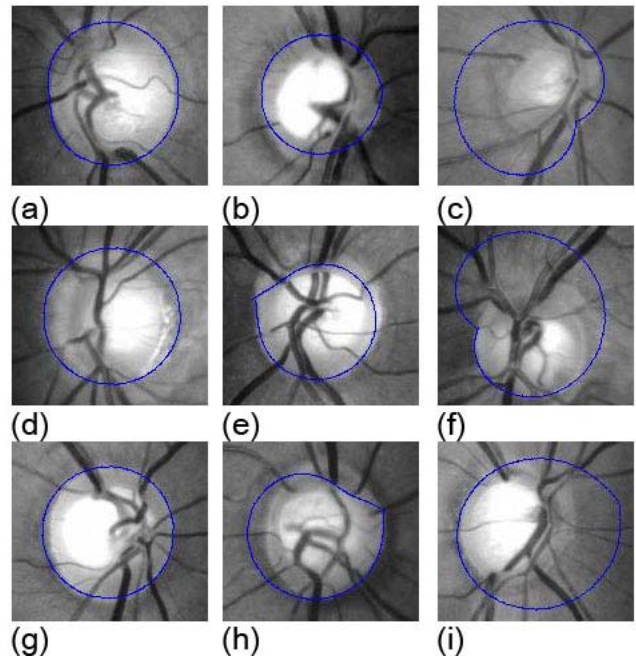

Fig. 7 Outlining of optic nerve head by machine, (a) (d) (g): good, (b) (e) (h): fair, (c) (f) (i): bad
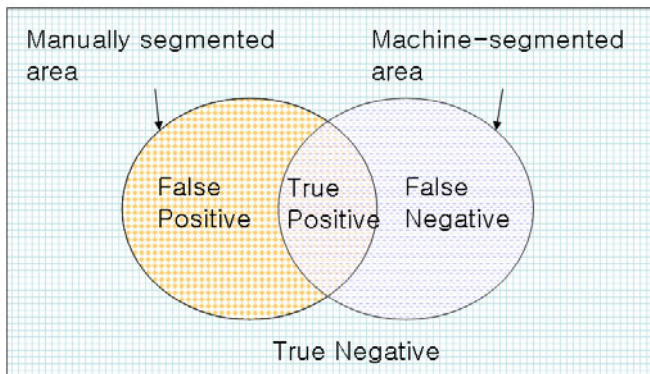
Fig. 8 Area of true positive, true negative, false positive and false negative

IV. DISCUSSION

Proposed algorithm was more robust than simple thresholding method, and showed better reproducibility than the segmentation method based on active contour. Through modeling of the boundary, segmentation of the optic nerve head becomes simple and explicit. This method will be helpful in improving the computerized analysis of the RNLFP for the computer-assisted evaluation of the glaucomatous change. To enhance the performance of the proposed method, constraint condition into the model selection of RANSAC will be added in the future.

ACKNOWLEDGMENT

REFERENCES

[1] H. A. Quigley, "Number of people with glaucoma worldwide," Br J Ophthalmol, vol. 80, pp. 389-93, May 1996.

[2] D. E. Singer, D. M. Nathan, H. A. Fogel, and A. P. Schachat, "Screening for diabetic retinopathy," Ann Intern Med, vol. 116, pp. 660-71, Apr 15 1992

[3] J. Lowell, A. Hunter, D. Steel, A. Basu, R. Ryder, E. Fletcher, and L. Kennedy, "Optic nerve head segmentation," IEEE Trans Med Imaging, vol. 23, pp. 256-64, Feb 2004.

[4] V. Badlani, M. Shahidi, A. Shakoor, D. P. Edward, R. Zelkha, and J. Wilensky, "Nerve fiber layer thickness in glaucoma patients with asymmetric hemifield visual field loss," J Glaucoma, vol. 15, pp. 275-80, Aug 2006.

[5] R. P. Galvao Filho, R. M. Vessani, and R. Susanna, Jr., "Comparison of retinal nerve fibre layer thickness and visual field loss between different glaucoma groups," Br J Ophthalmol, vol. 89, pp. 1004-7, Aug 2005

[6] F. Mendels, C. Heneghan, and J. P. Thiran, "Identification of the optic disk boundary in retinal images using active contours," Proceddings of the Irish Machine Vision and Image Processing Conference (IMVIP'99), pp. 103-115, 1999.

[7] H. Li and O. Chutatape, "Automated feature extraction in color retinal images by a model based approach," IEEE Trans Biomed Eng, vol. 51, pp. 246-54, Feb 2004.

[8] A. Osareh, M. Mirmehdi, B. Thomas, and R. Markham, "Comparison of colour spaces for optic disc localisation in retinal images," 2002, pp. 743-746 vol.1.

[9] H. J. Kong, J. M. Seo, S. Y. Lee, H. Chung, D. M. Kim, J. M. Hwang, K. S. Park, and H. C. Kim, "Quantification of progression of retinal nerve fiber layer atrophy in fundus photograph" The 3rd European Medical and Biological Engineering Conference, November 20-25 2005.

[10] M. A. Fischler and R. C. Bolles, "Random sample consensus: A paradigm for model fitting with applications to image analysis and automated cartography," Comm. Assoc. Comp. Mach., vol. 24, pp. 381-395, 1981

[11] R. I. Hartley and A. Zisserman, Multiple View Geometry in Computer Vision 2nd edition, Cambridge University Press, 2004